



The oxidation of a gasoline surrogate in the negative temperature coefficient region

David B. Lenhert^{a,1}, David L. Miller^{a,*}, Nicholas P. Cernansky^a, Kevin G. Owens^b

^a Department of Mechanical Engineering and Mechanics, Drexel University, 3141 Chestnut Street, Philadelphia, PA 19104-2875, USA

^b Department of Chemistry, Drexel University, 3141 Chestnut Street, Philadelphia, PA 19104-2875, USA

ARTICLE INFO

Article history:

Received 23 October 2006

Received in revised form 10 November 2008

Accepted 14 November 2008

Available online 26 January 2009

Keywords:

Autoignition

Surrogate

n-Heptane

Iso-octane

Toluene

1-Pentene

Flow reactor

ABSTRACT

This experimental study investigated the preignition reactivity behavior of a gasoline surrogate in a pressurized flow reactor over the low and intermediate temperature regime (600–800 K) at elevated pressure (8 atm). The surrogate mixture, a volumetric blend of 4.6% 1-pentene, 31.8% toluene, 14.0% *n*-heptane, and 49.6% 2,2,4-trimethyl-pentane (iso-octane), was shown to reproduce the low and intermediate temperature reactivity of full boiling range fuels in a previous study. Each of the surrogate components were examined individually to identify the major intermediate species in order to improve existing kinetic models, where appropriate, and to provide a basis for examining constituent interactions in the surrogate mixture. *n*-Heptane and 1-pentene started reacting at 630 K and 640 K, respectively, and both fuels exhibited a strong negative temperature coefficient (NTC) behavior starting at 700 and 710 K, respectively. Iso-octane showed a small level of reactivity at 630 K and a weak NTC behavior starting at 665 K. Neat toluene was unreactive at these temperatures. The surrogate started reacting at 630 K and exhibited a strong NTC behavior starting at 693 K. The extent of fuel consumption varied for each of the surrogate constituents and was related to their general autoignition behavior. Most of the intermediates identified during the surrogate oxidation were species observed during the oxidation of the neat constituents; however, the surrogate mixture did exhibit a significant increase in intermediates associated with iso-octane oxidation, but not from *n*-heptane. While neat toluene was unreactive at these temperatures, in the mixture it reacted with the radical pool generated by the other surrogate components, forming benzaldehyde, benzene, phenol, and ethyl-benzene.

The observed *n*-heptane, iso-octane, and surrogate oxidation behavior was compared to predictions using existing kinetic models. The *n*-heptane model reasonably predicted the disappearance of the fuel, but overpredicted the formation of several of the smaller intermediates. The iso-octane model significantly overpredicted the reaction of the fuel and formation of the intermediates. The 1-pentene model reasonably predicted the fuel consumption, but underestimated the importance of radical addition to the double bond. The results of this study provide a critical experimental foundation for the investigation of surrogate mixtures and for validation of kinetic models.

© 2008 The Combustion Institute. Published by Elsevier Inc. All rights reserved.

1. Introduction

Understanding the chemical processes that cause a fuel to autoignite is critical for solving the problem of knock in spark ignition engines and for the development of Low Temperature Combustion engine technologies such as Homogeneous Charge Compression Ignition (HCCI) and its derivatives. As the autoignition phenomena is strongly dependent on the oxidation chemistry of the hydrocarbon, which depends on the hydrocarbon structure and the temperature and pressure of the combustion environment,

a fundamental understanding of the low and intermediate temperature chemistry of the different hydrocarbon structural groups present in automotive fuels is necessary. With the increased interest in the effect of fuel formulations on controlling engine operations, extensive studies of the combustion of fuel-size hydrocarbons, neat and in mixtures, have been conducted over the past few years and the results have been recently reviewed [1,2]. No attempt will be made to repeat those reviews here; however, it is necessary to highlight certain studies of the reactivity of hydrocarbon mixtures to put the present work in proper perspective.

Leppard [3] examined the autoignition of binary blends of alkenes/alkanes in a motored engine to investigate the chemical origins of non-linear blending octane numbers. Stoichiometric mixtures of 2-butene/*n*-heptane and 1,3-butadiene/*n*-heptane were examined. The 2-butene/*n*-heptane mixture exhibited a significantly

* Corresponding author. Fax: +1 (215) 895 1478.

E-mail address: dmiller@coe.drexel.edu (D.L. Miller).

¹ Current address: Praxair Inc., 175 East Park Dr, Tonawanda, NY 14150, USA.

higher octane quality than neat *n*-heptane, but significantly lower than neat 2-butene. Furthermore, the intermediates formed exclusively from *n*-heptane occurred in the same relative concentrations as observed for neat *n*-heptane, however, this did not apply to the 2-butene intermediates. A similar phenomena was also observed for the 1,3-butadiene/*n*-heptane mixture. In the mixtures alkenes formed fewer cyclic ethers as intermediates than in neat oxidation and instead formed aldehydes. Leppard suggested that the interaction between the mixture constituents occurred only through small radicals, such as HO₂ and OH.

Vanhove et al. [4] investigated the autoignition of several stoichiometric mixtures in a rapid compression machine below 900 K, specifically, *n*-heptane/toluene, iso-octane/toluene, iso-octane/1-hexene, 1-hexene/toluene, and iso-octane/1-hexene/toluene blends. During the study, they measured ignition delay times and hydrocarbon intermediates at selected residence times after compression. Several significant differences between the *n*-heptane/toluene and iso-octane/toluene blends were observed. The addition of toluene to *n*-heptane reduced the overall reactivity and the temperature dependence of the reactivity. The addition of the toluene to iso-octane altered the phenomenology of the autoignition process by reducing the reactivity of the blend below 830 K and increasing the reactivity at higher temperatures. The three component mixture, a volumetric blend of 47% iso-octane, 18% 1-hexene, and 35% toluene, produced cool flame behavior. The conversion of the mixture components after the cool flame varied from 20% for toluene, 30% for iso-octane, and 35% for 1-hexene. The main products of the oxidation were consistent with the independent reaction of the “pure” hydrocarbons, not from any interaction of the components. However, due to the difficulty in quantifying the broad range of possible intermediate and final species produced during the oxidation of such a complex mixture, Vanhove et al. only accounted for approximately half of the carbon atoms.

Khan [5] formulated a surrogate mixture, 4.6% 1-pentene, 49.6% iso-octane, 14% *n*-heptane, and 31.8% toluene by volume, to have similar ratios of hydrocarbon functional groups, octane rating, and low and intermediate temperature reactivity as several industry standard full boiling range fuels, specifically RFA (Reference Fuel A) from the Auto/Oil Air Quality Improvement Research Program, indolene (the certification fuel) and a standard test fuel from Ford. The addition of 1-pentene and toluene to a *n*-heptane and iso-octane blend, reduced the overall reactivity, shifted the start of the Negative Temperature Coefficient (NTC), a region between 600 and 800 K where reactivity decreases as temperature increases, to higher temperatures in a flow reactor, and delayed the autoignition behavior in engines. A functional group analysis method was developed to use infrared absorption to provide semi-quantitative measurements of aromatics, alkenes, aldehydes, and alkanes from the flow reactor studies. Khan noted that the concentration of aromatics was nearly constant and concluded that toluene did not react in the low and intermediate temperature regime. However, as the infrared technique was tuned to aromatic ring structure, these results may have simply indicated that the ring did not open.

The present study expands on this research to elucidate the effects of the alkene and aromatic components in full boiling range fuels and to provide an experimental foundation for modeling surrogate mixtures. To this end the preignition chemistry of the individual components and gasoline surrogate mixture developed by Khan, referred to as GS4c-1, was examined by measuring the reacted gas composition at selected conditions.

2. Experimental facility

This study utilized the Drexel Pressurized Flow Reactor (PFR) Facility operating in the low and intermediate temperature regime (600–800 K) at an elevated pressure (8 atm) under dilute condi-

tions. The PFR facility was designed such that chemical processes could be examined in relative freedom from fluid mechanics and temperature gradient effects. A detailed description of the experimental facility and experimental techniques has been reported earlier [6–8] and only a summary is presented here. The key operational feature of the reactor is a quartz reactor tube within a pressure vessel. To achieve high reaction pressures, the inside of the quartz reactor and the annulus between it and the pressure vessel are maintained at the same pressure.

Nitrogen (purity >99.999%) and oxygen (purity >99.6%) were mixed into the PFR system to create a synthetic “air” mixture free of contaminants. This “oxidizer” stream was heated by in-line heaters to achieve the desired reaction temperatures. To maximize the temperature uniformity along the length of the reactor tube, two techniques were utilized. First, the fuel and oxidizer were diluted with nitrogen to limit the temperature rise due to heat release. For these experiments, the dilution was varied according to the reactivity of the fuel, specifically between 62–85%, where the dilution was defined as the volumetric flow of additional nitrogen divided by the volumetric flow of the synthetic “air” plus the additional nitrogen. Second, the walls of the pressure vessel were heated by three independently controlled resistive bead heaters. Using this combination of techniques, the initial temperature profile was isothermal to within 5 °C without reaction and 20 °C with reaction.

An independently controlled stream of heated nitrogen (purity >99.999%) was used to vaporize the fuel. The temperature of the nitrogen was controlled to a temperature 20–50 °C above the fuel vaporization temperature, as calculated from the Antoine equation [9]. The liquid fuel was injected into the centerline of the nitrogen stream by a high pressure syringe pump approximately one meter from the opposed jet mixing nozzle of the reactor. This provided sufficient time to vaporize the fuel completely and to remove any inhomogeneities. The syringe pump permitted accurate (within 0.5% of set point), repeatable, and stable delivery of liquid fuels, enabling day-to-day repeatability of CO concentrations (used for reactivity mapping) to less than 50 ppm during this study. To create the reactive mixture, the oxidizer stream and the pre-vaporized fuel/nitrogen stream were rapidly mixed in an opposed jet annular mixing nozzle at the entrance of the quartz reactor tube.

A water-cooled, glass-lined probe was used to extract samples from the centerline of the quartz reactor tube and to provide rapid quenching of chemical reactions. Sample temperatures were measured using a type-K thermocouple integrated into the probe assembly and extending 2.5 cm past the end of the probe tip. For the present experiments, the PFR was operated in a controlled cool down (CCD) mode to examine the reactivity over a range of temperatures at a fixed residence time and pressure, creating a “reactivity map” of the fuel. In this mode, the probe position along the centerline of the quartz tube is adjusted using a linear positioning table in order to maintain a fixed residence time as the reactor slowly cools (2–3 °C/min). The extracted gas samples were directed and split among online NDIR (non-dispersive infrared) analyzers for carbon monoxide (CO) and carbon dioxide (CO₂) measurements, a total hydrocarbon (THC) analyzer, and a multiple loop sample (MLS) storage system for offline analysis of up to 14 stored samples collected at selected reaction temperatures. The transfer lines and MLS system were heated to 120 °C to minimize condensation of the high boiling point hydrocarbons in the sample, specifically higher molecular weight species and oxygenated hydrocarbons.

The reactivity of the fuel, including NTC behavior, was determined through continuous monitoring of CO formation. This measurement has been shown to be a good measure of low and intermediate temperature reactivity, as CO does not oxidize significantly to CO₂ in this temperature regime [10].

Table 1
Summary of experimental conditions.

Fuel	Purity	Equivalence ratio	Dilution (%)	Residence time (ms)	Fuel concentration (ppm)	Carbon atoms
1-Pentene	>99%	0.51	70	175 ± 15 ms	4276	21380
<i>n</i> -Heptane	>99.7%	0.51	85	100 ± 7 ms	1459	10210
Iso-octane	>99.9%	1.0	62	250 ± 26 ms	6346	50760
Toluene	>99.5%	1.0	60	250 ± 26 ms	6435	45050
GS4c-1	–	0.73	65	225 ± 22 ms	C ₅ H ₁₀ : 232 C ₇ H ₁₆ : 705 C ₈ H ₁₈ : 2500 C ₇ H ₈ : 1602 Total: 5039	C ₅ H ₁₀ : 1160 C ₇ H ₁₆ : 4935 C ₈ H ₁₈ : 20000 C ₇ H ₈ : 11214 Total: 37309

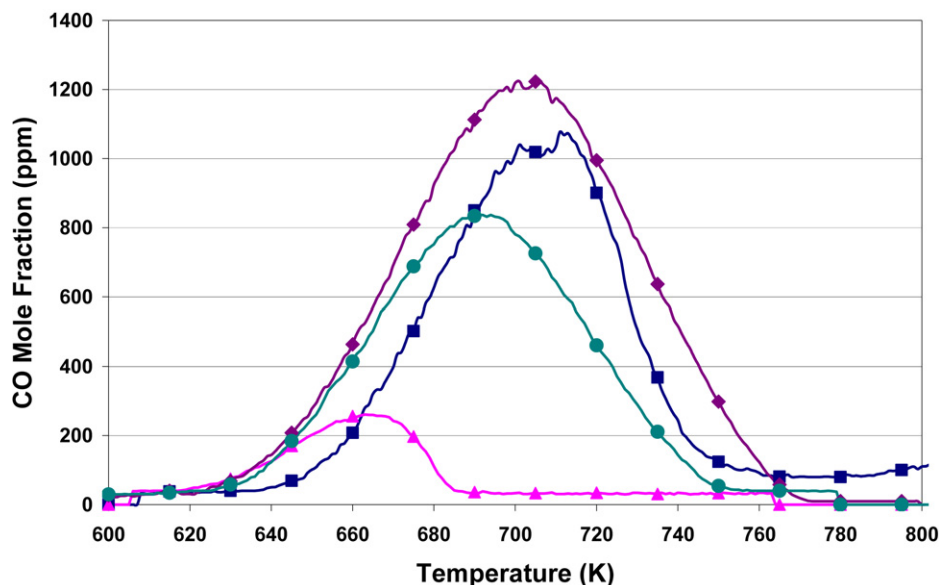


Fig. 1. Reactivity behavior of the gasoline surrogate and its components: (■) 1-Pentene; (▲) iso-octane; (◆) *n*-heptane; (●) surrogate (GS4c-1).

The offline analysis of the stable intermediate species was accomplished with a gas chromatograph (GC) with a flame ionization detector (FID) and a mass spectrometer (MS). For chromatographic separation, a Supelco Petrocol DH column (100 m, 0.5 μm film thickness, 0.25 mm OD) was utilized. The flow from the Petrocol DH column was split between the FID and MS detectors to permit simultaneous species quantification and identification. Identification of the unknowns was accomplished by retention time matching and/or by matching of the measured MS spectrum with the NIST '02 database (145,000+ unique compounds) [11]. Concentration of the identified compounds was determined primarily using the FID in the GC. Compounds, for which standards were not available, were quantified employing the calibration curve of a molecule with similar structure. Analysis of variance and regression analysis were employed to determine the errors associated with the quantification of the intermediate combustion species. The results of this analysis provided the uncertainty in any single value calculated from the calibration curve, and these are included in the graphs for the intermediates measured with the FID.

3. Experimental results

3.1. Reactivity mapping

The surrogate and its components were examined in the low and intermediate temperature regime at elevated pressure (8 atm). The specific equivalence ratio and dilution utilized was dependent on the reactivity of the fuel, and the specific values for these parameters were selected to limit heat release while achieving suf-

ficient reactivity for identification of the major intermediates. The specific conditions for each of the fuels are outlined in Table 1. Note that the uncertainty of residence time is the uncertainty in the absolute sampling time, while the relative uncertainty of residence times within a fuel experiment is a few milliseconds. Furthermore, the samples of the fuels were selected to be as pure as economically feasible to limit the possibility of impurities initiating reaction.

Under the conditions of the neat 1-pentene study, reactivity started at 640 K and CO concentration peaked, indicating the start of NTC behavior, at 710 K, Fig. 1. Neat *n*-heptane started reacting at 630 K and also exhibited a strong NTC behavior, observed to begin at 700 K. During the CCD experiments with 2,2,4-trimethylpentane (iso-octane), weak reactivity started at 630 K and NTC behavior was observed to begin at 665 K. The 40 °C lower temperature for the start of the NTC region for iso-octane, as compared to *n*-heptane, is intuitively backward for a fuel with a higher octane rating. However, the presence of the weaker tertiary bonded hydrogen in iso-octane allowed the initiation to occur at lower temperatures. Neat toluene was not reactive at the conditions examined.

For the surrogate mixture, GS4c-1, reactivity started at 630 K and NTC behavior was observed to begin at 693 K. Although comparing the start of the NTC region of the components with the surrogate is only strictly valid for identical conditions, higher concentrations should shift the start of the NTC region to higher temperatures. In these studies, the iso-octane was examined at a higher concentration relative to the surrogate mixture and 1-pentene was examined at a lower concentration. Considering the

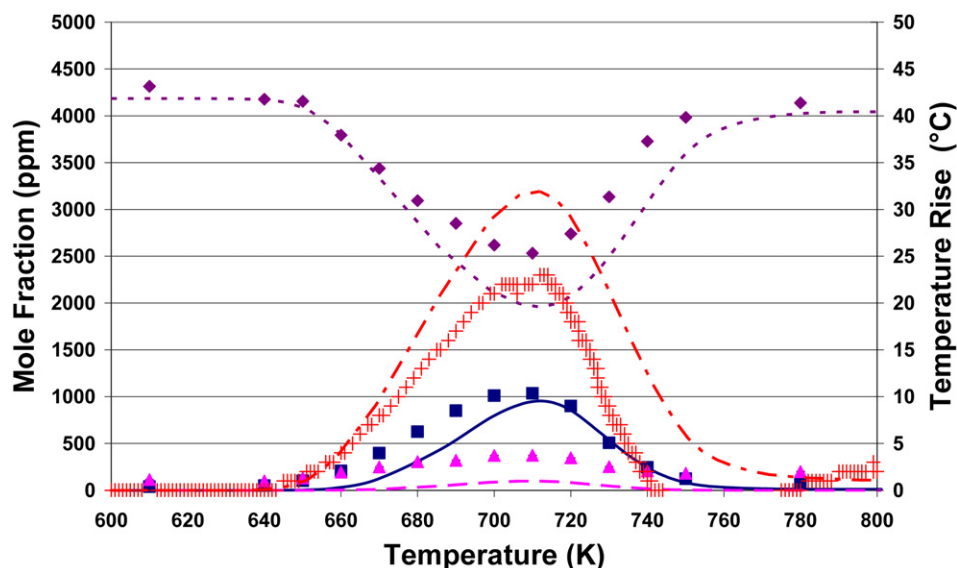


Fig. 2. Species profiles and temperature rise as a function of reactor temperature for 1-pentene (4276 ppm, $\phi = 0.51$, 70% dilution, 175 ms, and 8 atm): (■, —) CO; (▲, - -) CO₂; (◆, ·····) 1-pentene; (+, - - -) ΔT . Symbols are experimental results; lines are model predictions.

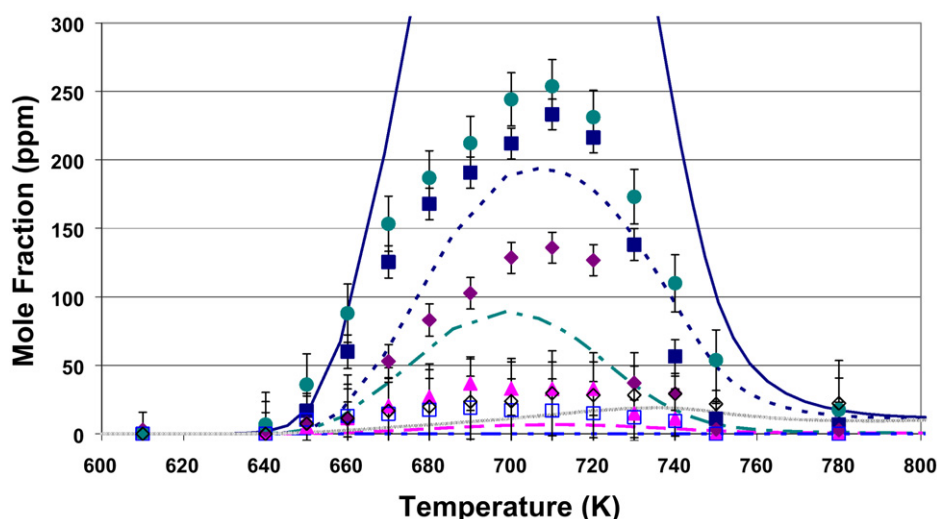


Fig. 3. Aldehyde and ether species profiles as a function of reactor temperature for 1-pentene (4276 ppm, $\phi = 0.51$, 70% dilution, 175 ms, and 8 atm): (■, —) Acetaldehyde; (▲, - -) propanal; (◆, ·····) 2-propenal; (●, — ·) butanal; (□, - - -) 2-pentenal; (◇, ·····) 2-propyl-oxirane. Symbols are experimental results; lines are model predictions.

concentration effect, the temperature for start of the NTC region for blends should be bound by the start of the NTC region for the individual components of that blend. A similar bounding was observed when comparing the gasoline primary reference fuels (PRF, *n*-heptane and iso-octane) and their blends, as the start of the NTC region for the PRF blends started near 687 K [1]. This bounding suggests that the addition of 1-pentene to the surrogate mixture could partially be responsible for the shift of the start of the NTC region to higher temperatures as compared to PRF blends. However, due to the low concentrations of 1-pentene in the surrogate mixture, it's more likely that the combination of 1-pentene and toluene's unreactive and radical scavenging nature resulted in the shift of the start of the NTC region.

3.2. 1-Pentene oxidation speciation results

Samples were collected at 14 temperatures during the 1-pentene reactivity mapping experiment to identify and quantify intermediate species in the low and intermediate tempera-

ture regime. The identified intermediates, signified by symbols in Figs. 2–4, accounted for 85% of the available carbon atoms (21380 C atoms). Note that this carbon balance only includes the carbon from positively identified compounds and does not include unidentified peaks of known molecular weight. Including these unidentified peaks, which MS fragmentation patterns suggest are mainly C₅ oxygenates, would increase the carbon balance to above 90%.

Also shown in Figs. 2–4 are species profiles calculated using the detailed kinetic model of Touchard et al. [12]. The mechanism contained 3385 elementary reactions among 837 chemical species. In this work, focusing on experimentally measuring the reactivity and reaction pathways of the selected hydrocarbons, no attempt was made to optimize or analyze the results of the model simulations. The simulations are presented primarily to indicate the state of our chemical understanding of the reactivity of these hydrocarbons.

The PFR was modeled in Chemkin 3.7.1 as an adiabatic plug flow reactor 40 cm long and 2.2 cm in diameter with no surface chemistry. The adiabatic representation of the reactor was chosen

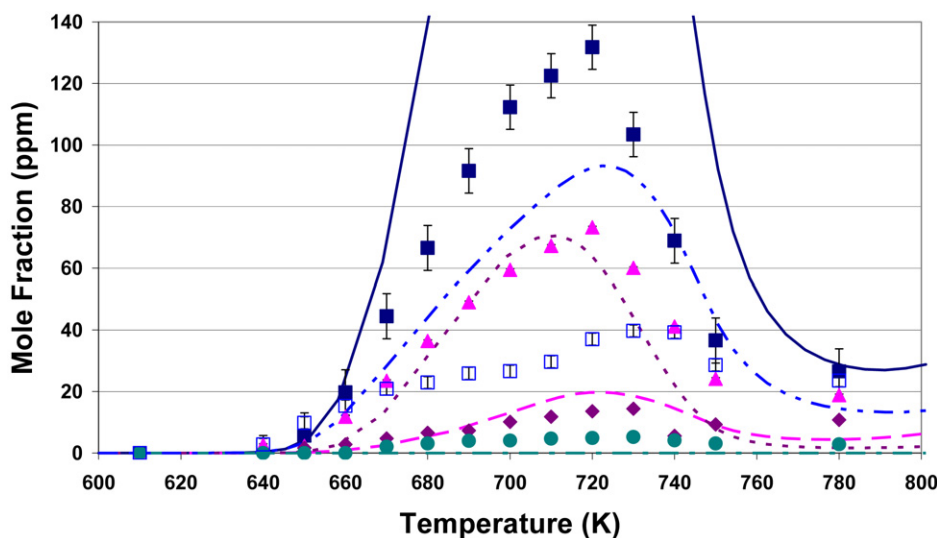


Fig. 4. Alkene species profiles as a function of reactor temperature for 1-pentene (4276 ppm, $\phi = 0.51$, 70% dilution, 175 ms, and 8 atm): (■, —) Ethene; (▲, - - -) 1-propene; (◆, ·····) 1,3-butadiene; (●, —) 2-pentene; (□, - - -) cis- and trans-1,3-pentadiene. Symbols are experimental results; lines are model predictions.

as some temperature rise occurred along the length of the reactor. The magnitude of the temperature rise can not be directly measured during the experiments but can be determined by comparing the time history of the actual sample temperature to that of a “non-reacting” sample temperature. The “non-reacting” temperature history was modeled as a second order polynomial and was tuned to the specific experimental conditions by removing temperatures where significant reactivity occurred during the experiment. Nominally, this procedure permitted estimation of the temperature rise to within a few degrees. Determination of this temperature rise can assist in assuring that nearly isothermal conditions are achieved and aid in modeling the specific temperature conditions in the flow reactor. One complication with modeling flow reactor data is that there is a finite physical mixing distance of the fuel and oxidizer streams and a thermal mixing distance due the fuel and oxidizer streams entering at two different temperatures, thus resulting in a “poorly” defined reaction time equals zero. As a result, flow reactor model predictions are often shifted in time to match the experiments at a specific condition. However, no time shift was applied to the simulated species profiles calculated in this study.

Fig. 2 presents the measured fuel mole fraction along with the measurements of CO, CO₂, and temperature rise. Slightly more than 40% of the fuel was converted to intermediate species of which CO and CO₂ formation accounted for more than 6% of the total initial carbon atoms (21380 C atoms) at the start of the NTC region. Large concentrations of aldehydes were formed during the oxidation of 1-pentene with butanal and acetaldehyde being the most abundant, Fig. 3. While not quantified by FID, large concentrations of formaldehyde were detected with the MS. Approximately 10% of the total initial carbon atoms were converted to aldehydes at their formation peak, which occurred at the same temperature as the start of the NTC region, 710 K. Inclusion of an estimate for formaldehyde, using the MS signal, would increase the overall aldehyde yield to over 16%. The temperature of the maximum concentration of the individual species also corresponded to the start of the NTC region, except for 2-pentenal which peaked at approximately 690 K. The only positively identified ether was 2-propyl-oxirane, Fig. 3. Alkene formation represented the only other functional group formed in appreciable amounts, and at their maximum accounted for 4% of the total initial carbon atoms. The major alkene intermediates formed, ethene, 1-propene, and 1,3-pentadiene, are presented in Fig. 4. Both of the 1,3-pentadiene iso-

mers were quantified, trans-1,3-pentadiene was the favored isomer producing twice the quantity of cis-1,3-pentadiene over most of the temperature range. Unlike the aldehydes, the alkene formation peaked at temperatures higher than the start of the NTC region. The peak of formation for the individual alkene species varied significantly. Of the major alkenes, both ethene and 1-propene had maximum formation around 720 K and rapidly declined at higher temperatures. 1,3-Pentadiene peaked at even higher temperatures, approximately 740 K, and its formation increased dramatically at the start of the NTC region.

The results suggest that there are two dominant pathways for the decomposition of 1-pentene, specifically, hydrogen abstraction of the allylic hydrogen and subsequent alkane type decomposition reactions [13,14] and radical addition to the double bond and decomposition through the “Waddington” mechanism [15,16]. As such, the abstraction of the allylic hydrogen and subsequent alkane type decomposition was responsible for the formation of 1,3-pentadiene, ethene, acetaldehyde, 2-propenal and other intermediates. If oxygen addition occurred at the allylic abstraction site followed by secondary hydrogen abstraction of a primary hydrogen (to form the alkene equivalent of the QOOH radical), then the preferred decomposition pathway was through the formation of a lower molecular weight alkene and aldehyde, not through the formation of a cyclic ether. The prominence of this pathway accounted for the equal portions of ethene and 2-propenal and low production of 2-ethenyl-oxetane (less than 2 ppm) in these experiments. However, if the secondary hydrogen abstraction removed the secondary hydrogen adjacent to the allylic hydrogen, then the dominant decomposition pathway was through addition of a second oxygen molecule to the radical site and subsequent decomposition to form acetaldehyde, the third most abundant species. The large concentrations of butanal and formaldehyde suggested that the Waddington mechanism was the dominant pathway for the decomposition of the fuel. However, studies by Stark and Waddington [17] and Prahbu et al. [18] have questioned its importance. Prahbu and coworkers observed an abundance of propanal and 2-methyl-tetrahydrofuran (THF) from the alkane type decomposition pathways, but did not measure butanal which is expected from the Waddington mechanism, and thus argued that the Waddington mechanism was not nearly as important as the alkane type hydrogen abstraction reactions for 1-pentene. However, propanal and 2-methyl-THF require the abstraction of a vinylic hydrogen, which requires approximately 6 kcal/mol more energy than secondary hy-

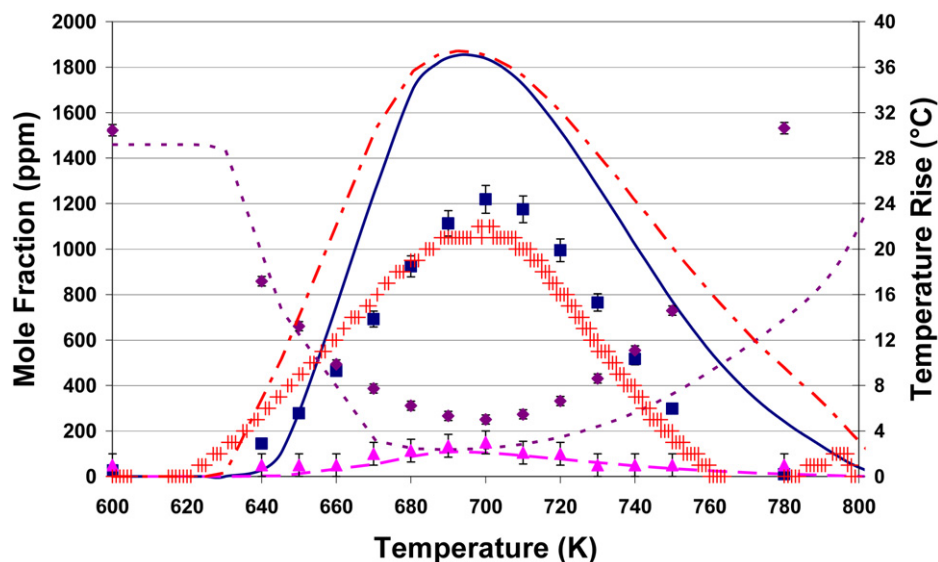


Fig. 5. Species profiles and temperature rise as a function of reactor temperature for *n*-heptane (1469 ppm, $\phi = 0.51$, 85% dilution, 100 ms, and 8 atm): (■, —) CO; (▲, - - -) CO₂; (◆, ·····) *n*-heptane; (+, - · - ·) ΔT . Symbols are experimental results; lines are model predictions.

drogen bonds. Prahbu offered no explanation as to why this larger energy barrier alkane pathway would dominate over other lower energy barrier alkane pathways. The experimental results of the present paper and that of Minetti et al. [19] both show elevated concentrations of butanal with significantly lower concentrations of propanal and 2-methyl-THF. This suggests that the abstraction of the vinylic hydrogen may not be as important as proposed by Prahbu. Further discussion of these competitive reaction steps is presented in the review of Battin-Leclerc [2].

In general, the comparisons between the Touchard model and experimental results were quite good. The adiabatic description for the PFR agreed reasonably well with the experimental temperature rise, albeit slightly overpredicting the temperature rise between 680 and 750 K, Fig. 2. However, the results do clearly demonstrate why the adiabatic model was chosen for this experiment over an isothermal model. The relatively minor overprediction of the temperature rise in the adiabatic representation of the reactor can partially explain the observed differences in fuel decomposition between the experiment and modeling. However, where the temperatures matched (<680 K), sizable differences in intermediates were observed. Specifically, the formation of CO, 1-propene, and butanal were under predicted and 1,3-butadiene was over predicted. The model also does not predict the rapid increase in 1,3-pentadiene formation as the temperature increases beyond the start of the NTC region. As noted previously, the formation of 1,3-pentadiene occurs through alkane type decomposition pathways. For *n*-heptane, a similar rapid increase was observed for the C₇ alkenes and ethers and attributed to the backward shift for the addition reaction of O₂ to heptyl and heptylhydroperoxy radicals (see below), suggesting that improvements could be made to the alkane type decomposition pathways in the 1-pentene mechanism. Furthermore, the mechanism tended to underestimate the formation of intermediates through the “Waddington” reaction pathway. Increasing the importance of the “Waddington” mechanism versus hydrogen abstraction of the allylic hydrogen may improve the model predictions presented here and in Minetti et al. [19].

As the alkene molecules become larger and there is larger separation between the double bond and the terminal methyl group, it is reasonable to assume radical addition to the double bond would become less important. It is important to establish the carbon chain length that produces the switch between the radical addition pathway and the alkane hydrogen abstraction pathways in

order to allow the simplification of the alkene decomposition pathways in the surrogate fuel mechanisms. The results presented here provide important experimental evidence as to the importance of the “Waddington” mechanism for alkenes in surrogate mixtures.

3.3. *n*-Heptane oxidation speciation results

The major intermediates were measured in samples extracted at 14 temperatures during the *n*-heptane reactivity mapping experiment. The identified intermediates, signified by symbols in Figs. 5–8, accounted for 60% of the available carbon atoms (10210 C atoms). MS fragmentation patterns indicate that the unidentified compounds were likely oxygenated intermediates, but they were not positively identified. Positive identification of these larger oxygenated compounds are very difficult, as they are not available for purchase nor are they included in the NIST MS database. Using the known molecular weights of the next 5 major intermediates would increase the carbon balance to over 80%. As with 1-pentene simulations using an existing detailed kinetic model are also plotted. The basic mechanism and thermochemistry by Curran et al. [13], 2450 elementary reactions among 550 chemical species, including updated chemical rate and thermodynamic parameters [20], was utilized for this comparison. Again, the PFR was modeled in Chemkin as an adiabatic plug flow reactor 40 cm long with a 2.2 cm diameter with no time shift or surface chemistry.

Fig. 5 illustrates the measured *n*-heptane disappearance along with the measurements of CO, CO₂, and temperature rise as a function of sample temperature. Over 80% of the initial fuel present was converted to intermediate species near the start of the NTC region, of which CO and CO₂ formation accounted for more than 13% of the total initial carbon atoms (10210 C atoms). Ethers were the most abundant functional group measured over much of the temperature range, Fig. 6. At temperatures lower than the start of the NTC region ether formation was roughly constant and accounted for 8% of the total initial carbon atoms. After the start of the NTC region, ether formation increased considerably to its peak of over 16% near 750 K. However, there were a significant number of ethers predicted by the mechanism that were not identified. The major ether identified was 2-methyl-5-ethyl-THF, Fig. 6. Both of the 2-methyl-5-ethyl-THF isomers were quantified, trans-2-methyl-5-ethyl-THF was the favored isomer producing 1.6 times the quantity of cis-isomer prior to the start of the NTC region and 1.3 times

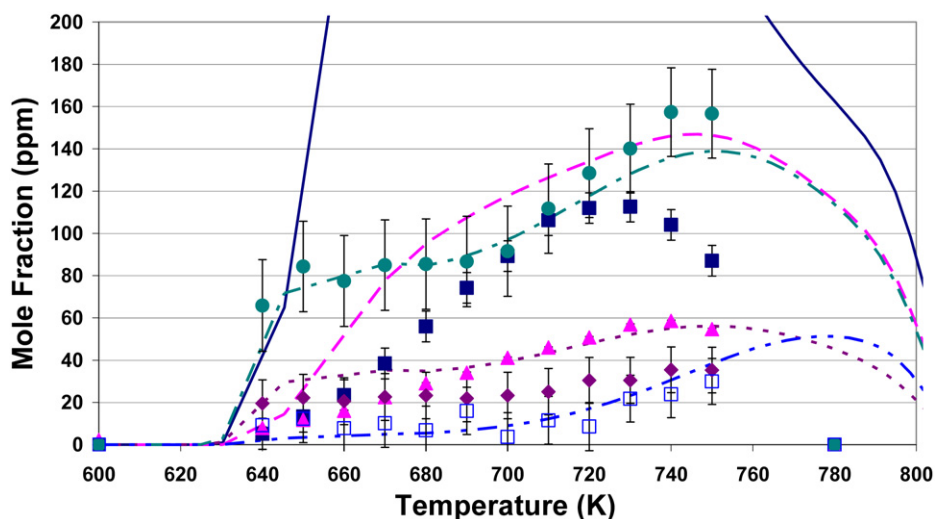


Fig. 6. Alkene and ether species profiles as a function of reactor temperature for *n*-heptane (1469 ppm, $\phi = 0.51$, 85% dilution, 100 ms, and 8 atm): (■, —) Ethene; (▲, —) 1-propene; (◆, —) 2-propyl-THF; (●, —) 2-methyl-5-ethyl-THF; (□, —) 2-methyl-4-propyl-oxetane. Symbols are experimental results; lines are model predictions.

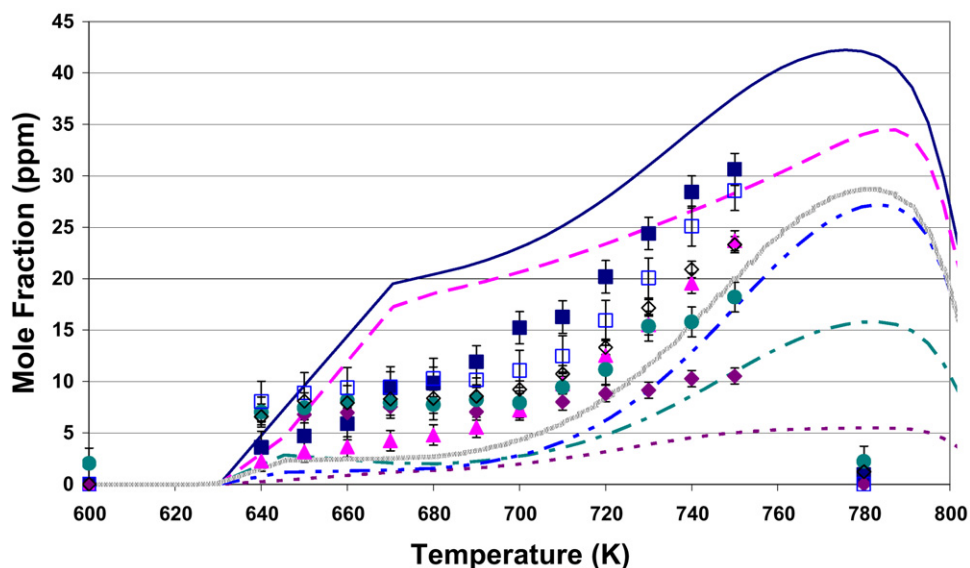


Fig. 7. Alkene profiles as a function of reactor temperature for *n*-heptane (1469 ppm, $\phi = 0.51$, 85% dilution, 100 ms, and 8 atm): (■, —) 1-Butene; (▲, —) 1-pentene; (◆, —) 1-hexene; (●, —) 1-heptene; (□, —) cis- and trans-2-heptene; (◇, —) trans-3-heptene. Symbols are experimental results; lines are model predictions.

in the NTC region. Alkenes (Figs. 6 and 7) were the second most abundant functional group over much of the experimental conditions, representing nearly 12% of the total initial *n*-heptane carbon atoms at its maximum with ethene and 1-propene being the most abundant. The alkene formation peaked at temperatures above the start of the NTC region, roughly 40 °C higher, similar to the ethers and 1-pentene results. The temperature of peak formation for the individual alkene species did not vary as much as in the 1-pentene oxidation. Most of the major alkenes peaked between 740 and 750 K, the most notable exception was ethene which peaked around 720 K. Almost all of conjugate alkenes were identified, the only exception was cis-3-heptene, because it eluted with *n*-heptane during GC analysis. Based on the measurements of the individual isomers of 2-heptene, trans-2-heptene was the favored isomer resulting in a 2:1 ratio over cis-2-heptene. Comparing the 2-heptene isomers to 1-heptene showed that the 2-heptene isomers were favored and the degree of preference increased steadily from 1.2 to 1.6 as the temperature increased to 750 K. Furthermore, comparing trans-2-heptene with trans-3-heptene showed that the

3-heptene isomer was favored slightly at a 1.3:1 ratio. This suggests that overall the 3-heptene isomer was the preferred conjugate alkene with 2-heptene being next most preferred. However, this was expected as the formation of 1-heptene requires the abstraction of a stronger primary hydrogen bond. A significant feature of the conjugate alkenes, and that of the C₇ ethers, was that their concentration rose significantly as the temperature increased beyond the start of the NTC region. This sudden increase coincided with a decrease in aldehyde concentration. These shifts were due to the backward shift of O₂ addition to heptyl (\dot{C}_7H_{15}) and heptylhydroperoxy ($\dot{C}_7H_{14}OOH$) radicals [21,22]. As the equilibrium shifts backward at the start of the NTC region, a larger fraction of \dot{C}_7H_{15} and $\dot{C}_7H_{14}OOH$ radicals were available to undergo alternative reactions. Hence, more conjugate alkenes are formed from the decomposition of \dot{C}_7H_{15} and more ethers are formed from the decomposition of $\dot{C}_7H_{14}OOH$.

Aldehyde formation ranged from 8 to 9% of the total initial carbon atoms for much of the temperature range examined with acetaldehyde and propanal reaching their peak at approximately

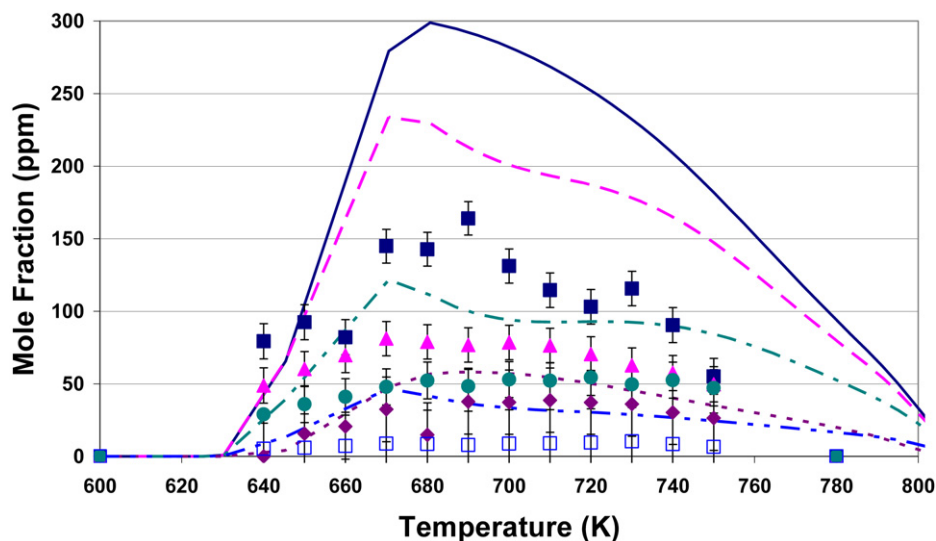


Fig. 8. Aldehyde profiles as a function of reactor temperature for *n*-heptane (1469 ppm, $\phi = 0.51$, 85% dilution, 100 ms, and 8 atm): (■, —) Acetaldehyde; (▲, - - -) propanal; (◆, ·····) 2-propanal; (●, - · - ·) butanal; (□, - - - -) pentanal. Symbols are experimental results; lines are model predictions.

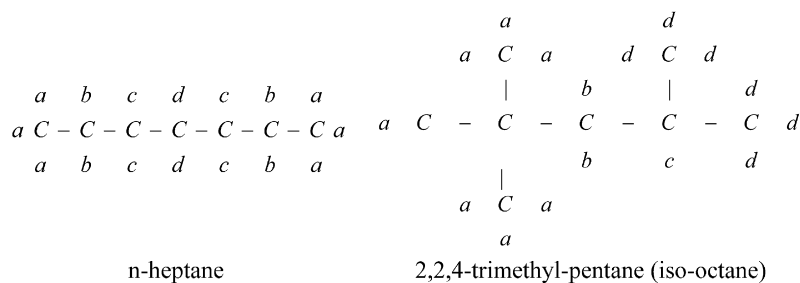


Fig. 9. Structure and H-abstraction sites of *n*-heptane and iso-octane.

680 K, Fig. 8. However, inclusion of a formaldehyde production estimate from the MS would increase the overall aldehyde yield to approximately 14% and the formation would peak at a temperature near the start of the NTC region. Unlike the aldehyde formation during 1-pentene oxidation, the individual aldehyde species formed during *n*-heptane oxidation were not as sensitive to temperature, as the profiles essentially rose to a plateau level over the range of experimental conditions. From a mechanistic perspective, two major pathways have been used to describe the formation of the aldehydes, specifically through the decomposition of the QOOH and OOQOOH radicals. The decomposition of the $\dot{C}_7H_{14}OOH$ radical would result in equal concentrations of lower molecular weight alkene and aldehyde pairs, for example 1-butene and propanal or 1-pentene and acetaldehyde. However, the concentrations of these aldehyde and alkene pairs were not measured in equal proportions. This suggests that the branching pathway decomposing the dihydroperoxyheptyl radical ($OO\dot{C}_7H_{14}OOH$) was the primary source of the aldehydes. Therefore, the two most abundant aldehydes, acetaldehyde and propanal, resulted from the decomposition of a $b\dot{C}_7H_{13}OO-bOOH$ radical and a $c\dot{C}_7H_{13}OO-cOOH$ radical, respectively, where the letters “b” and “c” indicate a distinct site for hydrogen abstraction, Fig. 9. The only exception for this dominant pathway for aldehyde formation is butanal. The equal proportions of butanal and 1-propene, the 6th and 7th most abundant species, indicate their formation was a result of the decomposition of the $d\dot{C}_7H_{14}OOH-b$ radical.

In general, the model predictions of *n*-heptane reaction were generally good, however, at temperatures above 670 K, the mechanism overpredicted the extent of fuel conversion. As with 1-pentene, the temperature rise with the adiabatic representation of

the reactor was higher than the experiments. After the start of the NTC region, the slope of the experimental and model temperature rise was nearly identical, however, the model predictions for fuel concentrations diverged significantly from the experiments. Specifically, the formation of the conjugate alkenes, Fig. 7, was underpredicted by approximately a factor of two, despite the overprediction of fuel disappearance. The most significant differences were observed in the lower molecular weight aldehydes and alkenes, namely ethene, acetaldehyde, and propanal. Nevertheless, the general trends and temperature dependence of the intermediate species were captured reasonably well. Perhaps most notable is the proper calculation of the trends for the ethers, Fig. 6, as there is a lack of data available to validate submechanisms describing their decomposition.

3.4. Iso-octane oxidation speciation results

Samples were only extracted and analyzed at 13 temperatures during the iso-octane (2,2,4-trimethyl-pentane) experiment. The identified intermediates, signified by symbols in Figs. 10–13, accounted for $100 \pm 3\%$ of the available carbon atoms (50760 C atoms). Several lower concentration intermediates, likely oxygenated intermediates, were not identified. If included in the carbon balance, they would not have had a significant impact on the overall carbon balance. As with *n*-heptane, the intermediate species profiles were compared to predictions using an updated version of a detailed iso-octane mechanism published by Curran et al. [20,23] containing 3600 elementary reactions among 860 chemical species. The higher initial iso-octane concentration along with the overprediction of the iso-octane reactivity from the model, re-

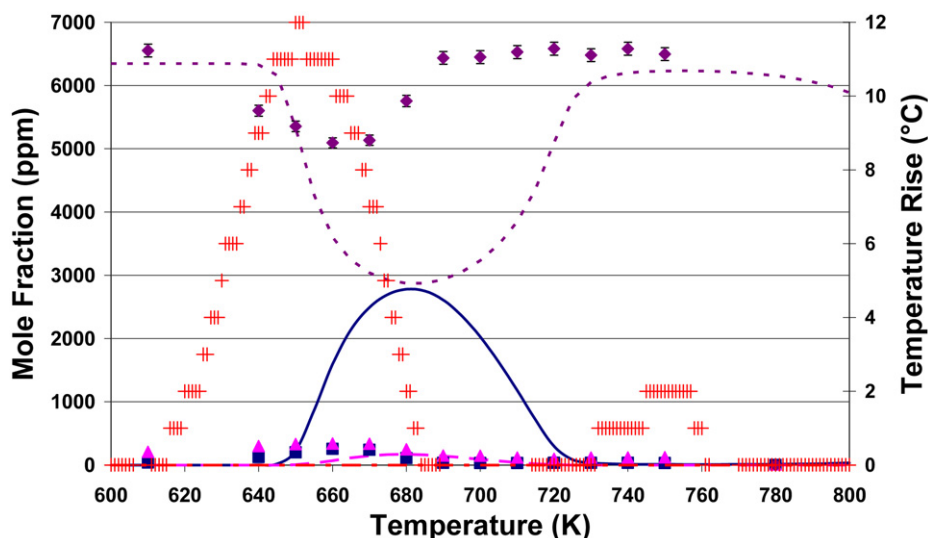


Fig. 10. Species profiles and temperature rise as a function of reactor temperature for iso-octane (6346 ppm, $\phi = 1.0$, 62% dilution, 250 ms, and 8 atm): (■, —) CO; (▲, —) CO₂; (◆, —) iso-octane; (+, —) ΔT . Symbols are experimental results; lines are model predictions.

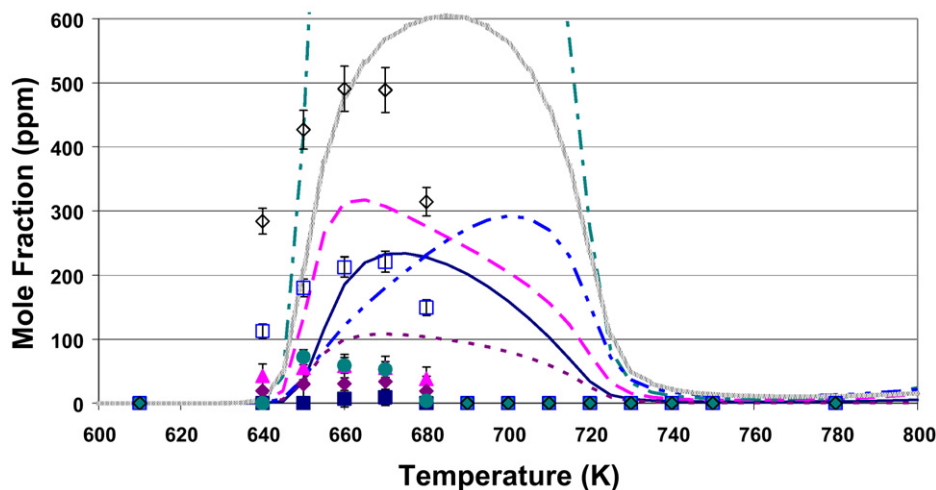


Fig. 11. Oxygenate species profiles as a function of reactor temperature for iso-octane (6346 ppm, $\phi = 1.0$, 62% dilution, 250 ms, and 8 atm): (■, —) Acetaldehyde; (▲, —) 2-methyl-propanal; (◆, —) 2,2-dimethyl-propanal; (●, —) 2-propanone; (□, —) 2-iso-propyl-3,3-dimethyl-oxetane; (◇, —) 2,2,4,4-tetramethyl-THF. Symbols are experimental results; lines are model predictions.

sulted in excessive heat release and temperature rise predictions using the adiabatic representation of the reactor. As a result, the isothermal representation was used as it provided a more realistic depiction of the experimental temperature profiles.

Fig. 10 shows the iso-octane mole fractions along with the measurements of CO, CO₂, and temperature rise as a function of sample temperature. Only 20% of the fuel was converted to intermediate species at the start of the NTC region. CO and CO₂ formation accounted for less than 1% of the total initial carbon atoms (50760 C atoms) at the start of the NTC region. The major class of intermediates formed before the start of the NTC region was ethers which account for over 11% of the total initial carbon atoms. The ether 2,2,4,4-tetramethyl-THF accounted for over 65% of the identified ethers, Fig. 11. A similar preferential formation of a single ether was also observed with *n*-heptane. Only a few aldehydes and ketones were identified with 2-propanone and acetaldehyde being the most abundant, Fig. 11. Aldehydes and ketones accounted for less than 2% and 1% of the total initial carbon atoms at the maximum, respectively. Inclusion of a formaldehyde production estimate would only increase the overall aldehyde yield to slightly more than 2%. Alkenes (Figs. 12 and 13) repre-

sented the second most abundant functional group to be formed over this temperature range and represented 4% of the total initial carbon atoms at its maximum with 2-methyl-1-propene and 2,4,4-trimethyl-1-pentene being the most abundant. The peak of the individual alkene species varied slightly, but most of the major alkenes peaked at roughly 670 K, the most notable exceptions were the methyl-1-pentenes that peaked around 660 K. Both of the 4,4-dimethyl-2-pentene isomers were observed with the *cis*-isomer formed at nearly 3.5 times the level of the *trans*-isomer.

Although *n*-heptane and iso-octane are both alkanes, they show significant differences in the preferred decomposition pathways. First, iso-octane produced significantly lower concentrations of aldehydes as compared to *n*-heptane. The dominant pathway for aldehyde formation with *n*-heptane required two internal hydrogen atom isomerizations. These isomerizations reactions are significantly slower in iso-octane due to its branched nature, resulting in the significantly lower concentrations of aldehydes. In *n*-heptane, the other dominant pathway for aldehyde formation occurred from the decomposition of the QOOH radical. This pathway tends to be more important in linear alkanes when the two abstraction sites are 2 carbon atoms away from each other, as indicated by the sig-

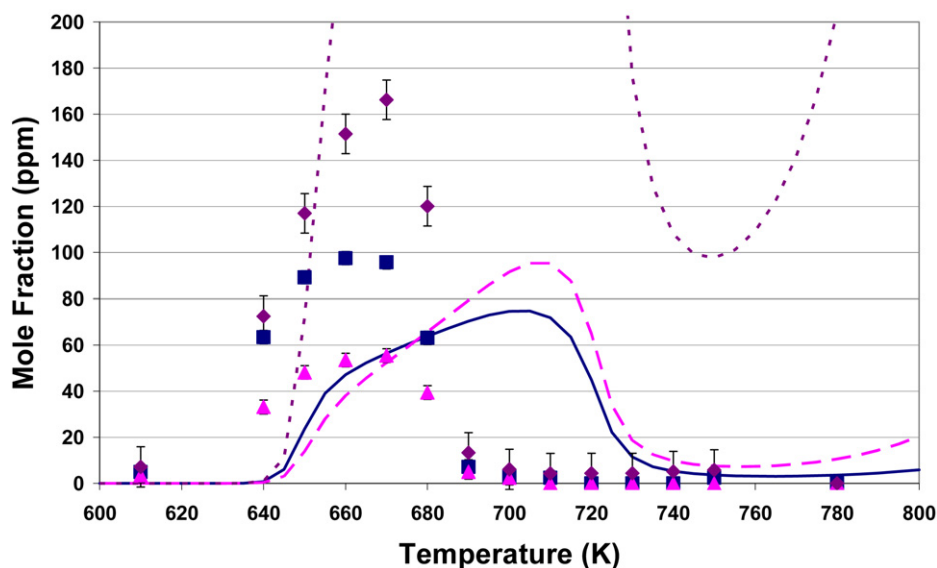


Fig. 12. Major alkene species profiles as a function of reactor temperature for iso-octane (6346 ppm, $\phi = 1.0$, 62% dilution, 250 ms, and 8 atm): (■, —) 2,2,4-Trimethyl-1-pentene; (▲, - - -) 2,2,4-trimethyl-2-pentene; (◆, ·····) 2-methyl-1-propene. Symbols are experimental results; lines are model predictions.

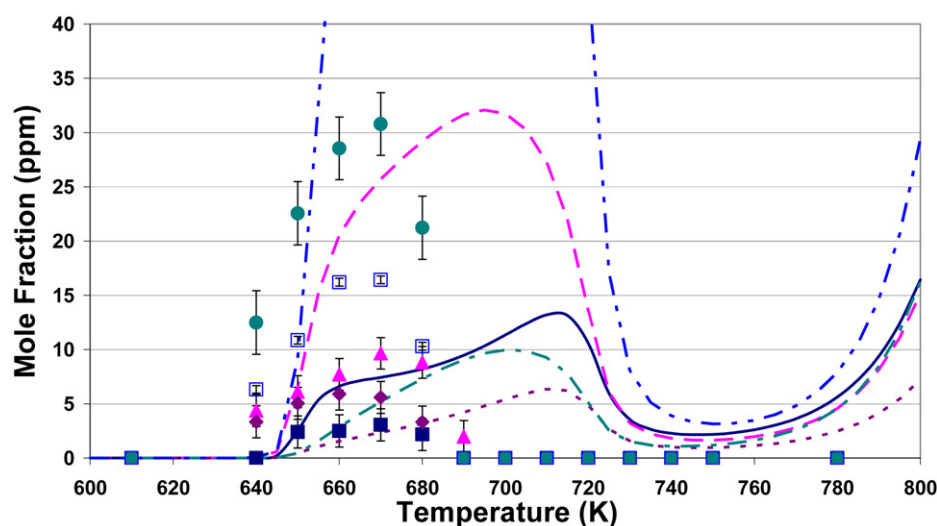


Fig. 13. Alkene species profiles as a function of reactor temperature for iso-octane (6346 ppm, $\phi = 1.0$, 62% dilution, 250 ms, and 8 atm): (■, —) 2,4-Dimethyl-1-pentene; (▲, - - -) 2,4-dimethyl-2-pentene; (◆, ·····) 4,4-dimethyl-1-pentene; (●, - · - ·) 4,4-dimethyl-2-pentene; (□, - - -) 1-propene. Symbols are experimental results; lines are model predictions.

nificant formation of butanal resulting from the decomposition of the $\dot{C}_7H_{14}OOH$ -b radical. This would suggest that the decomposition of the $\dot{a}C_8H_{16}OOH$ -b radical would tend to form an aldehyde. However, due to the branched structure of iso-octane, the preferred pathway was through the formation of an ether, specifically 2-isopropyl-3,3-dimethyl-oxetane. The consequence of these differences resulted in the reduced importance of aldehyde formation from iso-octane and an associated reduction in CO formation. Second, the relative importance of the individual conjugate alkenes for iso-octane were not ranked according to their activation energies. The formation of the conjugate alkenes, 2,4,4-trimethyl-1-pentene and 2,4,4-trimethyl-2-pentene, occurred from the internal isomerization of a $\dot{c}C_8H_{17}O\dot{O}$ radical. Either the “b” or “d” hydrogen must be abstracted to form the conjugate alkenes, since the “b” hydrogen is a secondary bonded hydrogen one would expect 2,4,4-trimethyl-2-pentene to be the favored species. However, three times the number of “d” hydrogen atoms compared to “b” hydrogen atoms resulted in the higher observed concentrations of 2,4,4-trimethyl-1-pentene over that of 2,4,4-trimethyl-2-pentene.

In general, the model predictions were very poor, significantly over estimating the decomposition of the fuel and formation of many of the intermediates. Specifically, the model overpredicted the formation of several lower molecular weight alkenes and oxygenates, namely 2-methyl-1-propene, 1-propene, and 2-propanone. Due to these significant discrepancies between model and experiment, the mechanism was examined to isolate pathways and intermediates which could, in part, account for the observed differences. The results suggest that the rate of secondary oxygen addition to the $\dot{C}_8H_{16}OOH$ radical may be overestimated. As a result, radicals such as $\dot{a}C_8H_{16}OOH$ -c and $\dot{a}C_8H_{16}OOH$ -b decompose to 2-propanone and 2-methyl-propanal rather than 2,2,4,4-tetramethyl-THF and 2-isopropyl-3,3-dimethyl-oxetane, respectively. This behavior would account for the overestimation of 2-propanone and 2-methyl-propanal and underestimation of 2,2,4,4-tetramethyl-THF and 2-isopropyl-3,3-dimethyl-oxetane. Consequently, the additional $\dot{d}C_8H_{16}OOH$ -c and $\dot{b}C_8H_{16}OOH$ -c radicals would result in an increase in 2,2,4-trimethyl-1-pentene and 2,2,4-trimethyl-2-pentene, which were also underestimated by the mechanism.

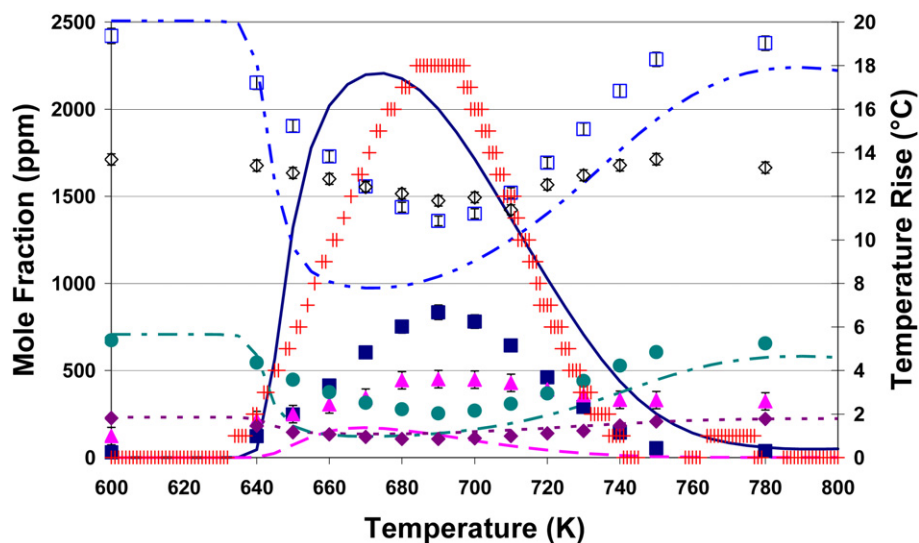


Fig. 14. Species profiles and temperature rise versus temperature for GS4c-1 (5039 ppm, $\phi = 0.73$, 65% dilution, 225 ms, and 8 atm): (■, —) CO; (▲, - - -) CO₂; (◆, ·····) 1-pentene; (●, —) *n*-heptane; (□, - - -) iso-octane; (◇) toluene, and (+) ΔT . Symbols are experimental results; lines are model predictions.

3.5. Surrogate mixture oxidation speciation results

Reaction gas samples were collected at 14 temperatures during the experiments with GS4c-1. The identified intermediates, signified by symbols in Figs. 14, 16–21, accounted for better than 90% of the available carbon atoms (37309 C atoms). This carbon balance only includes the carbon from positively identified compounds and does not include unidentified peaks of known molecular weight. Including these unidentified peaks was estimated to account for an additional 5–7% of the carbon atoms. A detailed chemical model which is able to model the surrogate mixture over the conditions of this experiment was not available in the open literature. A particular problem is that there is a complete lack of a toluene mechanism for lower temperatures [2]. Therefore, the intermediate species profiles were compared to predictions using a detailed chemical model for *n*-heptane/iso-octane oxidation published by Curran et al. [20,24] containing 4200 elementary reactions among 1050 chemical species and which includes a basic 1-pentene sub-mechanism. This mechanism was recently used to model homogeneous charge compression ignition (HCCI) engines with reasonable success [25]. The initial conditions for the surrogate mixture were modified to include only the mole fractions of *n*-heptane, iso-octane, and 1-pentene, with nitrogen substituted for the mole fraction of toluene. This substitution allowed the isolation of the effects of toluene addition on the surrogate mixture, discussed below. As with iso-octane, the isothermal representation was used as it provided a more realistic depiction of the experimental temperature profiles as the kinetic model significantly overpredicted fuel consumption and energy release.

Fig. 14 presents the measured fuel mole fractions and measurements of CO, CO₂, and temperature rise, along with the associated model predictions. The fractional consumption of the individual constituents in the surrogate varied significantly, Fig. 15, and is related to their respective research octane numbers (RON). Over 60% of the *n*-heptane (RON = 0) was converted to intermediates, while only 45% of the iso-octane (RON = 100) was converted. The peak of fuel consumption occurred at the start of the NTC region for both of these fuels and coincided with the overall maximum in fuel consumption. The measurement of 1-pentene (RON = 91) included the 1-pentene produced from *n*-heptane oxidation. To correct for the effects of this production, an estimate of the amount of 1-pentene produced from *n*-heptane was based upon the ratio of 1-pentene to *n*-heptane for the neat fuel study. Scaling

this ratio to the surrogate mixture concentrations suggested that a maximum of 12 ppm, or approximately 5% of the initial 1-pentene, would be produced from *n*-heptane reaction in the surrogate mixture. Furthermore, the maximum formation of 1-pentene occurred at a temperature higher than the start of the NTC region during the neat *n*-heptane study. This explains why the maximum percent consumption of 1-pentene shown in Fig. 15 is at a temperature lower than the start of the NTC region, 680 K. Toluene (RON = 120) measurements exhibited an anomalous behavior during the CCD experiments and during separate Constant Inlet Temperature (CIT) experiments (not shown here). During the fuel calibration, toluene would be measured in the proper percentages based upon the surrogate composition and reaction conditions, but when samples were quantified under an oxidizing environment approximately 10% more toluene was present than expected. Although some of the intermediates from *n*-heptane and iso-octane would coelute with toluene at conditions of high *n*-heptane and iso-octane reactivity, these intermediates are not significant under low reactivity conditions, specifically, the 600 K and 780 K sample points, where the difference was also observed. It is unclear what caused the variation in observed concentrations. Despite this discrepancy, the difference still shows that over 14% of the toluene was consumed and the peak reactivity occurred at the start of the NTC region.

Slightly more than 35% of the surrogate fuel was converted to intermediate species of which CO and CO₂ formation accounted for approximately 3% of the total initial carbon atoms (37309 C atoms) at the start of the NTC region. Ethers represented the most abundant functional group formed over the temperature range investigated and represented a maximum of approximately 10% of the total initial carbon atoms, Fig. 16. The ethers attributable to *n*-heptane decomposition were 2-methyl-5-ethyl-tetrahydrofuran (THF) and 2-propyl-THF, and those attributable to iso-octane decomposition were 2,2,4,4-tetramethyl-THF and 2-isopropyl-3,3-dimethyl-oxetane. The major ether formed by 1-pentene, 2-propyl-oxirane, was not quantified as it coeluted with iso-octane. The peak in the rate of formation for the 2-methyl-5-ethyl-THF isomers occurred at 720 K, approximately 30 °C after the start of the NTC region. The maximum concentration of both of the C₈ ethers coincided with the start of the NTC region.

Aldehyde formation peaked near 5% of the total initial carbon atoms, the major intermediates are shown in Figs. 17 and 18. While not quantified by FID, large concentrations of formaldehyde were

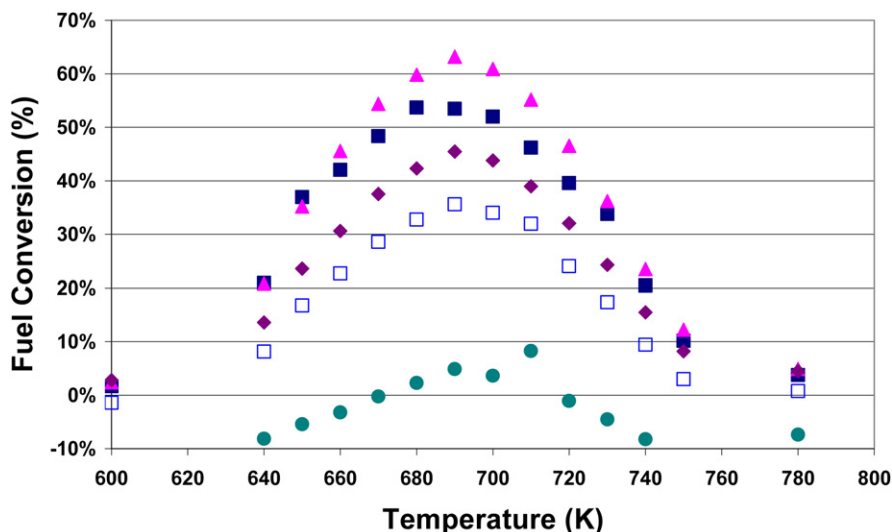


Fig. 15. Overall fuel conversion and conversion of the individual components for GS4c-1: (■) 1-Pentene; (▲) *n*-heptane; (◆) iso-octane; (●) toluene; (□) overall fuel conversion; (◇) carbon balance.

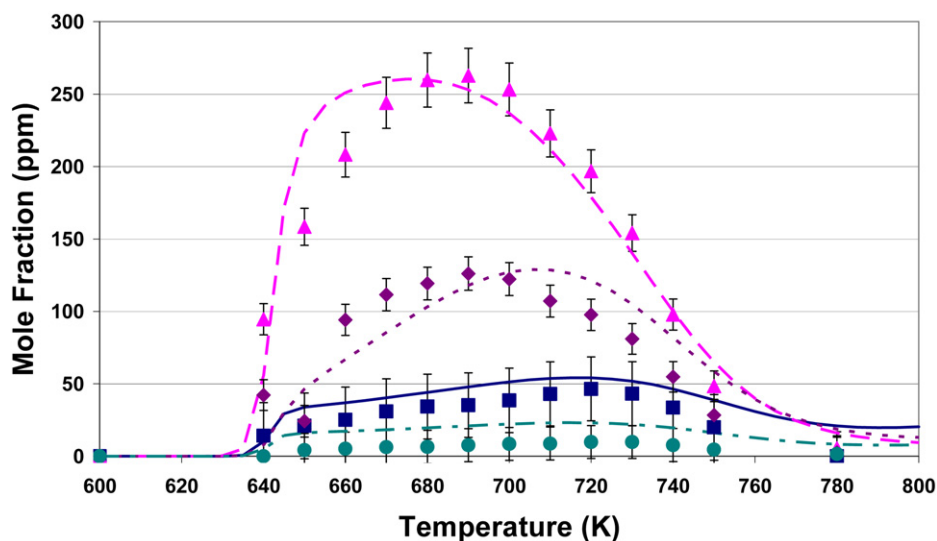


Fig. 16. Ether species profiles as a function of reactor temperature for GS4c-1 (5039 ppm, $\phi = 0.73$, 65% dilution, 225 ms, and 8 atm): (■, —) 2-Methyl-5-ethyl-THF; (▲, - - -) 2,2,4,4-tetramethyl-THF; (◆, ····) 2-isopropyl-3,3-dimethyl-oxetane; and (●, —) 2-propyl-THF. Symbols are experimental results; lines are model predictions.

detected with the MS. Using the MS signal and associated calibration curve for propanal; the concentration of formaldehyde can be estimated. Inclusion of this estimate would increase the overall aldehyde yield to approximately 6.5%. The aldehydes attributable to the reaction of *n*-heptane, iso-octane, and 1-pentene were the most abundant, specifically, formaldehyde and acetaldehyde. More interesting are measurements of aldehydes specific to a particular fuel component, notably, iso-octane reaction produced 2-methyl-propanal and 2,2-dimethyl-propanal and *n*-heptane produced pentanal. The other linear aldehydes are possibly produced from both *n*-heptane and 1-pentene consumption.

Alkene formation represented the third most abundant functional group over much of the temperature regime accounting for more than 4% of the total initial carbon atoms at its maximum, Figs. 19 and 20. The alkene formation peaked at a temperature 10 °C higher than the start of the NTC region. The peak of formation of the individual alkene species varied, but most of the major alkenes peaked at or above the start of the NTC region. Similar to neat iso-octane, 2,4,4-trimethyl-1-pentene in the surrogate mixture

peaked prior to the start of the NTC region, 680 K. Significant concentrations of alkenes specific to a particular fuel component were identified, particularly, iso-octane produced 2-methyl-1-propene, 2,4,4-trimethyl-1-pentene, and 2,4,4-trimethyl-2-pentene and *n*-heptane produced *cis*- and *trans*-2-heptene, and *trans*-3-heptene. Intermediates produced by 1-pentene, notably 1,3-butadiene and 1,3-pentadiene, were only identified at trace levels. Vanhove and coworkers [4] noted that 1-hexene produced a relatively larger concentration of hexadiene for their surrogate mixture. However, due to the significantly lower concentration of alkene used for the surrogate in this study, this phenomena was not observed for 1-pentene.

During the oxidation of the surrogate, three major species were quantified that could only be produced from toluene, specifically, benzaldehyde, benzene, and phenol, Fig. 21. Benzaldehyde represented the most abundant ring species accounting for over 7% of the total initial carbon atoms in toluene (11214 C atoms). Phenol and benzene were produced in nearly identical concentrations and accounted for approximately 1% of the total initial car-

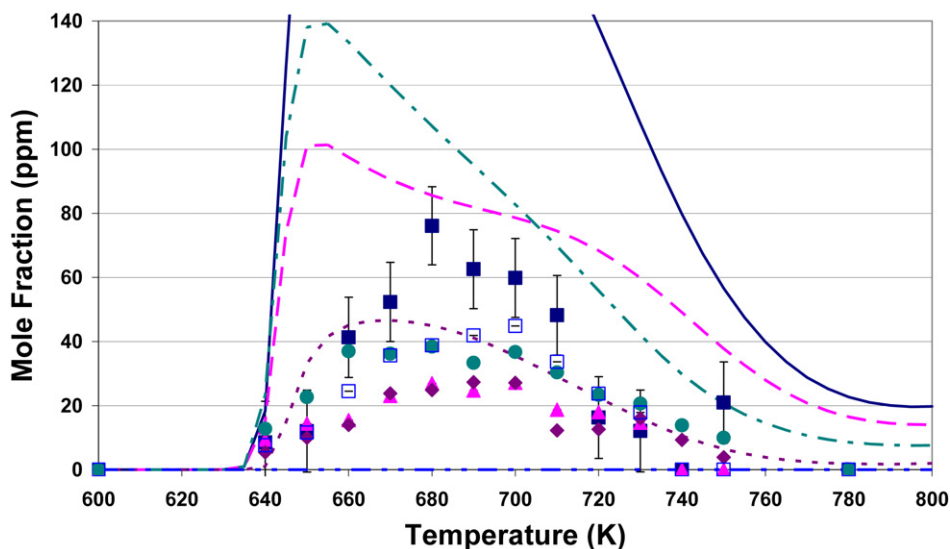


Fig. 17. Aldehydes species profiles as a function of reactor temperature for GS4c-1 (5039 ppm, $\phi = 0.73$, 65% dilution, 225 ms, and 8 atm): (■, —) Acetaldehyde; (▲, - - -) propanal; (◆, ·····) 2-propanal; (●, - · - ·) 2-methyl-propanal; and (□, —) 2-methyl-2-propanal. Symbols are experimental results; lines are model predictions.

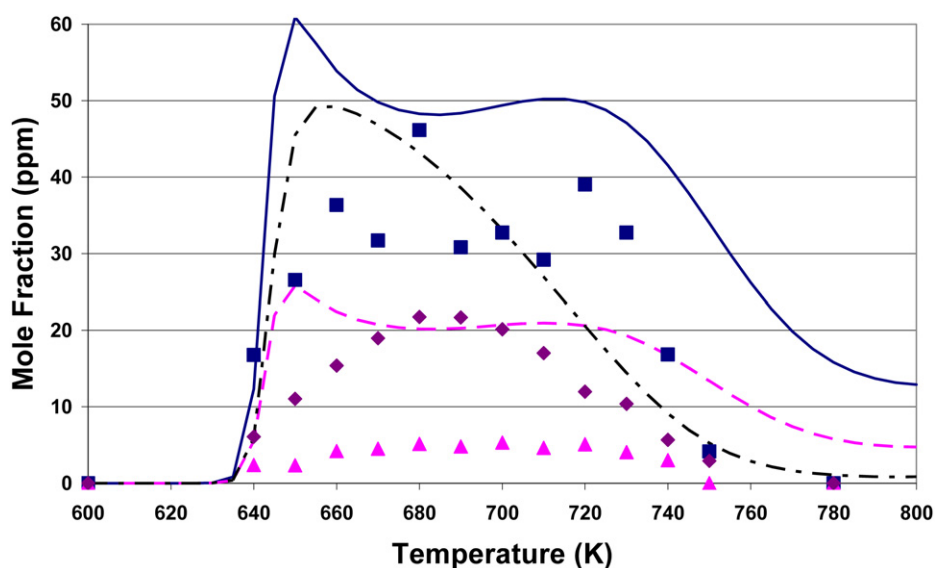


Fig. 18. Aldehydes species profiles as a function of reactor temperature for GS4c-1 (5039 ppm, $\phi = 0.73$, 65% dilution, 225 ms, and 8 atm): (■, —) Butanal; (▲, - - -) pentanal; and (◆, ·····) 2,2-dimethyl-propanal. Symbols are experimental results; lines are model predictions.

bon atoms in toluene. Due to the complexity of the gas mixture and the possibility of coelution of toluene reaction intermediates, the chromatograms were scrutinized for additional aromatics that were observed in previous studies [4,26–28], e.g., ethylbenzene, ethenylbenzene (styrene), benzyl alcohol, benzoic acid, dibenzyl, and methylbutenylbenzene. Ethylbenzene was identified but not quantified as it coeluted with 2-isopropyl-3,3-dimethyl-oxetane. However, species such as benzyl alcohol, and benzoic acid, and other hydrocarbons with boiling points above 450 K, were not identified due to chromatographic limitations. To determine if benzaldehyde, benzene, and phenol were the principal species resulting from the oxidation of the toluene and the extent of possible ring rupture, a carbon “ring balance” was determined. The “ring balance” ranged from 110% to 95% at the start of the NTC region. The apparent ring creation was an artifact of the previously mentioned variation in the toluene concentration between the fuel calibration step and the experiments. The completeness of the “ring balance” suggested that the aromatic ring structure

remained intact throughout the low temperature regime. In experiments at slightly higher temperatures, Dagaut et al. [29] suggested that a key decomposition pathway for phenyl radicals was through cyclopentadienyl, which will form 1,3-cyclopentadiene. No 1,3-cyclopentadiene was identified although the chromatographic technique could measure this compound, further suggesting that the ring structure remained intact.

4. Discussion

Several significant differences were observed between the neat hydrocarbon experiments and the surrogate mixture experiment. First, the marked increase in the 2-methyl-5-ethyl-THF concentration observed for neat *n*-heptane was not observed for the surrogate, rather the surrogate mixture produced a nearly steady increase in concentration to 720 K, Fig. 16. This suggested that the buildup of heptyl (C_7H_{15}) and heptylhydroperoxy ($C_7H_{14}OOH$) radicals was slower with the surrogate mixture. The fact that the

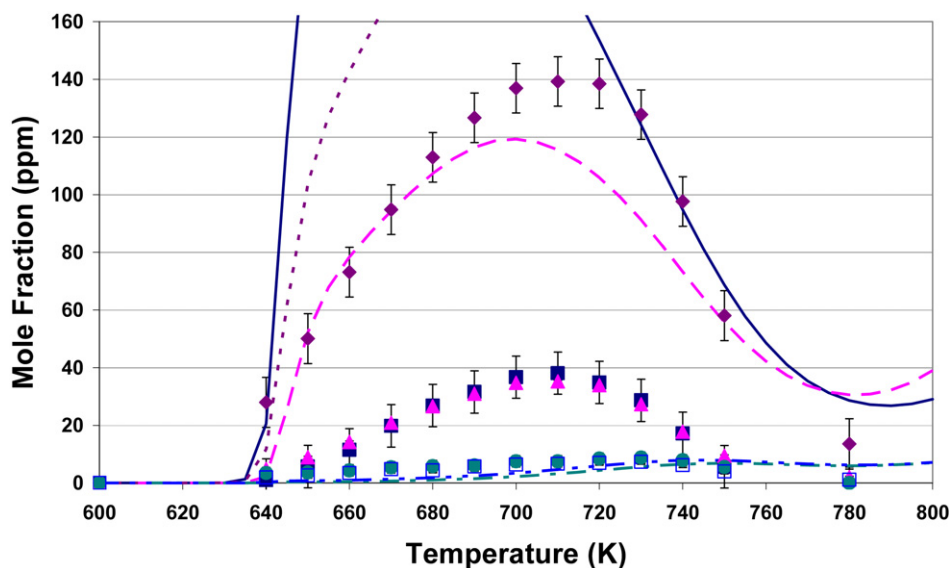


Fig. 19. Alkene species profiles as a function of reactor temperature for GS4c-1 (5039 ppm, $\phi = 0.73$, 65% dilution, 225 ms, and 8 atm): (■, —) Ethene; (▲, - - -) 1-propene; (◆, ·····) 2-methyl-1-propene; (●, — · —) cis- and trans-2-heptene; and (□, - - -) trans-3-heptene. Symbols are experimental results; lines are model predictions.

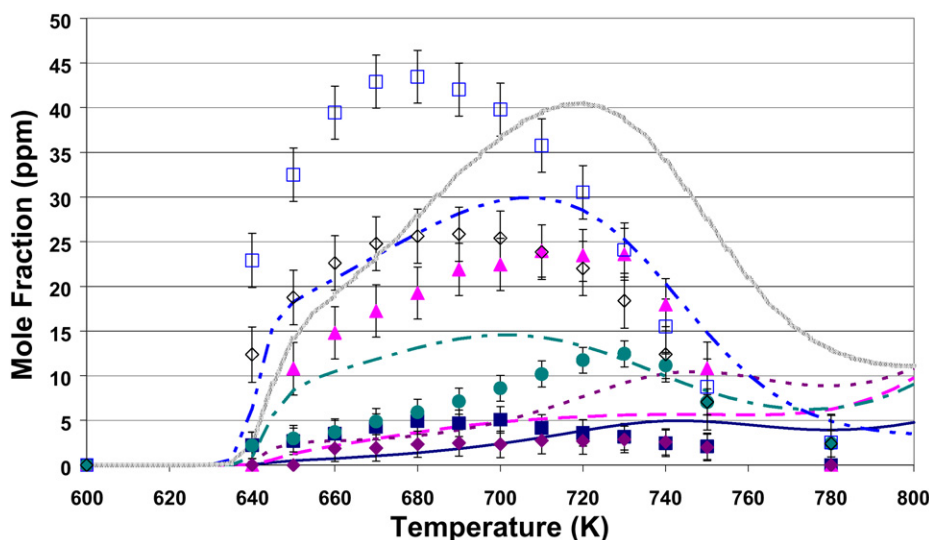


Fig. 20. Alkene species profiles as a function of reactor temperature for GS4c-1 (5039 ppm, $\phi = 0.73$, 65% dilution, 225 ms, and 8 atm): (■, —) 4,4-Dimethyl-1-pentene; (▲, - - -) 4,4-dimethyl-2-pentene; (◆, ·····) 2,4-dimethyl-1-pentene; (●, — · —) 2,4-dimethyl-2-pentene; (□, - - -) 2,4,4-trimethyl-1-pentene; and (◇, — · —) 2,4,4-trimethyl-2-pentene. Symbols are experimental results; lines are model predictions.

model predicted this behavior further suggests that the toluene addition was not responsible for this change. Furthermore, the relative production of two 2-methyl-5-ethyl-THF isomers in the mixture was more complicated than for the case of neat *n*-heptane. At the lowest temperatures, specifically 640 and 650 K, the trans-isomer was only slightly favored. Between 660 and 700 K, the relative formation of the trans-isomer increased to 1.6:1, the same ratio observed during the neat studies. At temperatures above 700 K, the preference for the trans-isomer decreased to a 1.3:1 ratio. This shift in the relative formation of the isomers coincided with the start of the NTC region, 700 K, in the neat studies, yet, for the mixture the change in the relative formation of the isomers did not shift to lower temperatures as the start of NTC region had shifted. Secondly, the relative importance of several of the intermediates changed significantly between the neat and surrogate mixtures. To allow comparison between the surrogate mixture and the neat

compounds, select species were identified that are only products of a single component. For each identified species, the concentration of that species was multiplied by its number of carbon atoms and then normalized by the initial number of carbon atoms from the fuel component that was responsible for the identified species formation, either neat or in the surrogate mixture. The comparison of this value, herewith referred to as “carbon fraction,” was made between the neat and surrogate mixtures at the same temperatures during the experiments. In addition, this carbon fraction was also calculated and compared for the model predictions for the neat and surrogate mixtures to isolate how residence time and equivalence ratio differences between the neat and surrogate mixture effected the observed changes. For iso-octane the comparisons were made at 670 K for 2,2,4,4-tetramethyl-THF, 2-isopropyl-3,3-dimethyl-oxetane, 2-methyl-propanal, 2,2-dimethyl-propanal, 2-methyl-1-propene, 2,2,4-trimethyl-1-pentene, and 2,2,4-trimethyl-

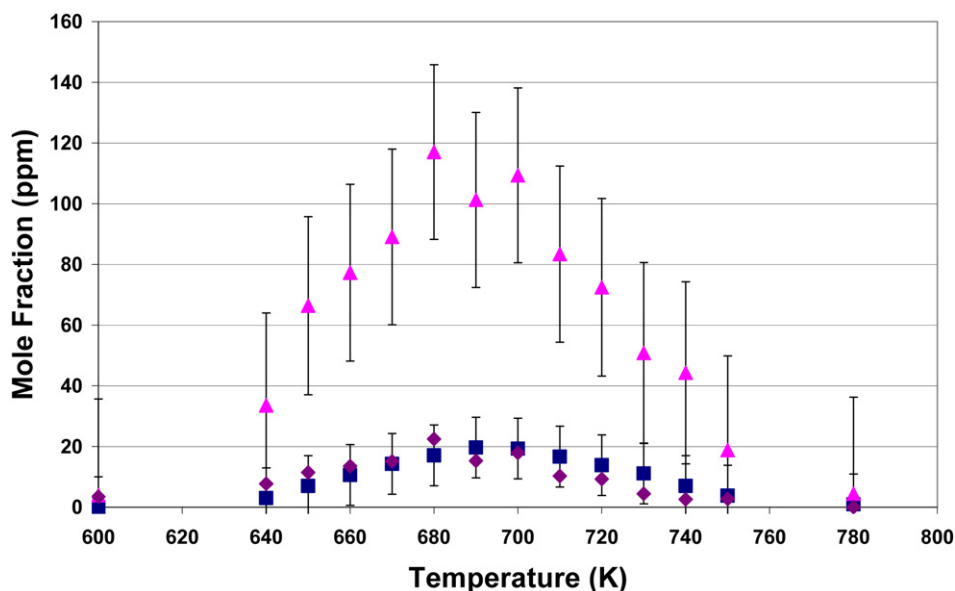


Fig. 21. Toluene intermediate species profiles as a function of reactor temperature for GS4c-1 (5039 ppm, $\phi = 0.73$, 65% dilution, 225 ms, and 8 atm): (■) Benzene; (▲) benzaldehyde; and (◆) phenol.

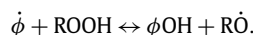
2-pentene. For *n*-heptane the comparisons were made at 700 K for 2-methyl-5-ethyl-THF, 2-propyl-THF, *cis*- and *trans*-2-heptene, and *trans*-3-heptene.

For the iso-octane experiment, the measured carbon fraction of 2,2,4,4-tetramethyl-THF, 2-isopropyl-3,3-dimethyl-oxetane, 2-methyl-propanal, and 2,2-dimethyl-propanal increased significantly by 29%, 31%, 70%, and 45%, respectively, for the surrogate mixture. The experimental carbon fraction for the alkenes produced from iso-octane also showed a sizable increase, 2-methyl-1-propene, 2,2,4-trimethyl-1-pentene, and 2,2,4-trimethyl-2-pentene increased 48%, 16%, and 16%, respectively. However, when the increases in the experimental carbon fractions were compared to the predicted carbon fractions, a significant difference was observed. The model predicted more modest increases in carbon fraction of 16%, 20%, 21%, 4%, and 12% for 2,2,4,4-tetramethyl-THF, 2-isopropyl-3,3-dimethyl-oxetane, 2-methyl-1-propene, 2,2,4-trimethyl-1-pentene, and 2,2,4-trimethyl-2-pentene, respectively. However, the formation of the iso-octane derived aldehydes showed the most significant differences between the experimental and modeling carbon fraction as the model only predicted a 9% increase in 2,2-dimethyl-propanal and no significant change in 2-methyl-propanal.

For *n*-heptane, the experimental carbon fraction for 2-methyl-5-ethyl-THF and 2-propyl-THF decreased 11% and 22%, and *cis*- and *trans*-2-heptene and *trans*-3-heptene increased 42% and 44%, respectively. Due to the low concentrations of pentanal, the effect on the aldehydes of *n*-heptane could not be inferred. However, the model predicted carbon fractions indicated that 2-methyl-5-ethyl-THF, 2-propyl-THF, 2-heptene, and 3-heptene should all increase, specifically, 7%, 13%, 51%, and 60%, respectively. As shown, the most significant differences in the measured and predicted carbon fractions occurred with the aldehydes formed from iso-octane and the ethers formed from *n*-heptane. This suggests that the addition of 1-pentene and toluene may affect branched and linear alkanes differently. It also suggests that some key interactions are not accounted for in the mechanism. Although speculative, these interactions may include co-oxidation reactions between iso-octane and *n*-heptane as suggested by Andrae et al. [30] or an effect associated with toluene addition.

As noted previously, one of the most significant observations with this study was the characterization of the reaction of toluene with the other surrogate components and the formation of aro-

matic intermediates. Several pathways have been proposed to explain toluene oxidation in the low and intermediate temperature regimes. Specifically, Ciajola et al. [31] suggested several pathways to form benzaldehyde and benzene during their oxidation of *n*-heptane/toluene mixtures. Vanhove et al. [4] proposed pathways to produce ethyl-benzene and methylbutenylbenzene and other co-oxidation reactions. However, neither study observed phenol. Although speculative, the following pathways could explain the formation of phenol.



In the surrogate mixture, there are significant concentrations of $\dot{\text{O}}\text{H}$ produced from aldehydes which could easily react with the long lived phenyl radicals ($\dot{\phi}$). This termination step would have a significant influence on the abstraction reactions from both alkanes and alkenes and on $\dot{\text{O}}\text{H}$ addition to the double bonds of alkene, as they are sensitive to $\dot{\text{O}}\text{H}$ concentrations. The second proposed reaction results in the formation of an alkoxy radical. The alkoxy radicals are unstable and rapidly decompose to form smaller, stable oxygenated species, principally aldehydes and ketones, and smaller alkyl radicals. These smaller alkyl radicals then tend to undergo β -scission to form even smaller alkyl radicals and alkenes. As a result, an increase in aldehyde formation and alkenes should be observed with the addition of toluene. The experimental results did show an increase in aldehyde formation as compared to model predictions, lending some credence to the proposed pathways. Vanhove and coworkers have suggested that interaction between the long lived radicals formed during toluene reaction and other larger radicals. However, the interactions between these larger radicals were not observed during this study. Nevertheless, this study clearly shows that toluene actively reacts in the low and intermediate temperature regimes with the radical pool generated by the other compounds.

5. Summary and conclusions

The oxidation of a proposed gasoline surrogate was investigated to examine the interaction of the constituents when examining the surrogate mixture. The gasoline surrogate was a mixture of 4.6% 1-pentene, 49.6% iso-octane, 14% *n*-heptane, and 31.8% toluene. Each

of the constituents was examined individually, nominally from 600 to 800 K at a pressure of 8 atm under dilute conditions. Both, 1-pentene and *n*-heptane showed a very strong NTC behavior, where the start of NTC occurred at 710 K and 703 K, respectively. Iso-octane also exhibited NTC behavior which started at 665 K. Toluene was not reactive at the conditions examined. The surrogate exhibited a strong negative temperature coefficient (NTC) behavior which started at 693 K. Comparing the reactivity behavior of the surrogate components with a surrogate mixture suggests that the temperature for start of the NTC region for blends should be bound by the start of the NTC region for the individual components of that blend.

Detailed speciation was completed throughout the NTC temperature range to identify and quantify the major intermediates species. For 1-pentene, the results showed that the fuel reacts through both alkane and alkene type pathways producing significant concentrations of formaldehyde, butanal, acetaldehyde, ethene, 2-propenal, and 1-propene. The preferred alkene type pathway was through HO₂ addition to the double bond, the “Waddington” mechanism, which was responsible for the formation of significant quantities of butanal and formaldehyde. The preferred alkane type pathways were through abstraction of the allylic hydrogen and subsequent decomposition. For *n*-heptane, over 80% of the fuel decomposed to intermediates at the start of the NTC region and produced significant concentrations of formaldehyde, acetaldehyde, 2-methyl-5-ethyl-THF, ethene, propanal, and butanal. For iso-octane, only 20% of the fuel decomposed to intermediates at the start of the NTC region and produced 2,2,4,4-tetramethyl-THF, 2-isopropyl-3,3-dimethyl-oxetan, formaldehyde, 2-methyl-1-propene, 2-propanone, and 2-methyl-propanal. For the surrogate, the carbon balance was very good (>90%) considering the complexity of the mixture. Most of the intermediates identified were the same as those present in the neat studies. Comparisons between the concentrations of the intermediate species in the surrogate and neat component experiments showed that iso-octane produced significantly more aldehydes, alkenes, and ethers in the mixture, while the *n*-heptane intermediates did not change significantly. This implies that the addition of 1-pentene and toluene may affect linear and branched alkanes differently. During the oxidation of the surrogate, over 14% of the toluene reacted to intermediates while no reactivity was observed with neat toluene. These intermediates appeared to retain the aromatic ring structure as no linear alkenes indicative of ring rupture were identified. Four major species were attributable to toluene decomposition, specifically, benzaldehyde, benzene, phenol, and ethyl-benzene. Two new pathways have been suggested to account for the formation of the phenol, which has not been observed previously in toluene studies.

Acknowledgments

This research was supported by the U.S. Army Research Office under ARO Contracts DAAG55-98-1-0286 and DAAD19-03-1-0070.

References

- [1] J.M. Simmie, Prog. Energy Combust. Sci. 29 (2003) 599–634.
- [2] F. Battin-Leclerc, Prog. Energy Combust. Sci. 34 (2008) 440–498.
- [3] W.R. Leppard, SAE Paper 922325, 1992.
- [4] G. Vanhove, G. Petit, R. Minetti, Combust. Flame 145 (3) (2006) 521–532.
- [5] A.R. Khan, M.Sc. thesis, Drexel University, Philadelphia, PA, 1998.
- [6] D.N. Koert, Ph.D. dissertation, Drexel University, Philadelphia, PA, 1990.
- [7] D.N. Koert, N.P. Cernansky, Meas. Sci. Technol. 3 (6) (1992) 607–613.
- [8] D.B. Lenhart, Ph.D. dissertation, Drexel University, Philadelphia, PA, 2004.
- [9] National Institute of Standards and Technology, NIST Chemistry WebBook, <http://webbook.nist.gov/chemistry/>.
- [10] D.N. Koert, D.L. Miller, N.P. Cernansky, Combust. Flame 96 (1–2) (1994) 34–49.
- [11] National Institute of Standards and Technology, NIST Standard Reference Database 1A, <http://www.nist.gov/srd/nist1a.htm>.
- [12] S. Touchard, R. Fournet, P.A. Glaude, V. Warth, F. Battin-Leclerc, G. Vanhove, M. Ribaucour, R. Minetti, Proc. Combust. Inst. 30 (2005) 1073–1081.
- [13] H.J. Curran, P. Gaffuri, W.J. Pitz, C.K. Westbrook, Combust. Flame 114 (1–2) (1998) 149–177.
- [14] P.A. Glaude, F. Battin-Leclerc, R. Fournet, V. Warth, G.M. Côme, G. Scacchi, Combust. Flame 122 (4) (2000) 451–462.
- [15] D.J.M. Ray, D.J. Waddington, J. Am. Chem. Soc. 90 (25) (1968) 7176–7178.
- [16] D.J. Waddington, D.J.M. Ray, Combust. Flame 21 (3) (1973) 327–334.
- [17] M.S. Stark, D.J. Waddington, Int. J. Chem. Kinet. 27 (1995) 123–151.
- [18] S.K. Prabhu, R.K. Bhat, D.L. Miller, N.P. Cernansky, Combust. Flame 104 (4) (1996) 377–390.
- [19] R. Minetti, A. Roubaud, E. Therssen, M. Ribaucour, L.R. Sochet, Combust. Flame 118 (1–2) (1999) 213–220.
- [20] Lawrence Livermore National Laboratory, LLNL Combustion Chemistry Group, http://www-cms.llnl.gov/combustion/combustion_home.html.
- [21] A. Ciajolo, A. D’Anna, Combust. Flame 112 (4) (1998) 617–622.
- [22] S.W. Benson, Thermochemical Kinetics, John Wiley and Sons, New York, 1976.
- [23] H.J. Curran, P. Gaffuri, W.J. Pitz, C.K. Westbrook, Combust. Flame 129 (3) (2002) 253–280.
- [24] H.J. Curran, W.J. Pitz, C.K. Westbrook, C.V. Callahan, F.L. Dryer, Proc. Combust. Inst. 27 (1998) 379–387.
- [25] M. Sjöberg, J.E. Dec, Proc. Combust. Inst. 30 (2005) 2719–2726.
- [26] J.A. Barnard, V.J. Ibberson, Combust. Flame 9 (1) (1965) 81–87.
- [27] J.A. Barnard, V.J. Ibberson, Combust. Flame 9 (2) (1965) 149–157.
- [28] R. Sivaramakrishnan, R.S. Tranter, K. Brezinsky, Combust. Flame 139 (4) (2004) 340–350.
- [29] P. Dagaut, G. Pengloan, A. Ristori, Phys. Chem. Chem. Phys. 4 (10) (2002) 1846–1854.
- [30] J. Andrae, D. Johansson, P. Björnborn, P. Risberg, G. Kalghatgi, Combust. Flame 140 (4) (2005) 267–285.
- [31] A. Ciajolo, A. D’Anna, R. Mercogliano, Combust. Sci. Technol. 90 (5–6) (1993) 357–371.

Public Reporting burden for this collection of information is estimated to average 1 hour per response, including the time for reviewing instructions, searching existing data sources, gathering and maintaining the data needed, and completing and reviewing the collection of information. Send comment regarding this burden estimate or any other aspect of this collection of information, including suggestions for reducing this burden, to Washington Headquarters Services, Directorate for Information Operations and Reports, 1215 Jefferson Davis Highway, Suite 1204, Arlington, VA 22202-4302, and to the Office of Management and Budget, Paperwork Reduction Project (0704-0188), Washington, DC 20503.

1. AGENCY USE ONLY (Leave Blank)		2. REPORT DATE 2/12/2009	3. REPORT TYPE AND DATES COVERED Technical Report, 2004	
4. TITLE AND SUBTITLE The oxidation of a gasoline surrogate in the negative temperature coefficient region			5. FUNDING NUMBERS Contract No. DAAD19-03-1-0070, Proposal No. 44458-EG	
6. AUTHOR(S) D.B. Lenhart, D.L. Miller, N.P. Cernansky, K.G. Owens				
7. PERFORMING ORGANIZATION NAME(S) AND ADDRESS(ES) Drexel University, 3141 Chestnut Street, Philadelphia, PA 19104			8. PERFORMING ORGANIZATION REPORT NUMBER	
9. SPONSORING / MONITORING AGENCY NAME(S) AND ADDRESS(ES) U. S. Army Research Office P.O. Box 12211 Research Triangle Park, NC 27709-2211			10. SPONSORING / MONITORING AGENCY REPORT NUMBER	
11. SUPPLEMENTARY NOTES The views, opinions and/or findings contained in this report are those of the author(s) and should not be construed as an official Department of the Army position, policy or decision, unless so designated by other documentation.				
12 a. DISTRIBUTION / AVAILABILITY STATEMENT Approved for public release; distribution unlimited.			12 b. DISTRIBUTION CODE	
13. ABSTRACT (Maximum 200 words) This experimental study investigated the preignition reactivity behavior of a gasoline surrogate in a pressurized flow reactor over the low and intermediate temperature regime (600-800 K) at elevated pressure (8 atm). The surrogate mixture, a volumetric blend of 4.6% 1-pentene, 31.8% toluene, 14.0% n-heptane, and 49.6% 2,2,4-trimethyl-pentane (iso-octane), was shown to reproduce the low and intermediate temperature reactivity of full boiling range fuels in a previous study. Each of the surrogate components were examined individually to identify the major intermediate species in order to improve existing kinetic models, where appropriate, and to provide a basis for examining constituent interactions in the surrogate mixture. Most of the intermediates identified during the surrogate oxidation were species observed during the oxidation of the neat constituents; however, the surrogate mixture did exhibit a significant increase in intermediates associated with iso-octane oxidation, but not from n-heptane. While neat toluene was unreactive at these temperatures, in the mixture it reacted with the radical pool generated by the other surrogate components, forming benzaldehyde, benzene, phenol, and ethyl-benzene. The results of this study provide a critical experimental foundation for the investigation of surrogate mixtures and for validation of kinetic models.				
14. SUBJECT TERMS Autoignition, Surrogate, n-Heptane, iso-Octane, Toluene, 1-Pentene, Flow reactor			15. NUMBER OF PAGES 16	
			16. PRICE CODE	
17. SECURITY CLASSIFICATION OR REPORT UNCLASSIFIED	18. SECURITY CLASSIFICATION ON THIS PAGE UNCLASSIFIED	19. SECURITY CLASSIFICATION OF ABSTRACT UNCLASSIFIED	20. LIMITATION OF ABSTRACT UU	